Indian J Med Res 159, May 2024, pp 479-493
DOI: 10.25259/ijmr_1262_22

Quick Response Code:

Clinical implications of activation of the *LIMD1-VHL*-HIF1α pathway during head-&-neck squamous cell carcinoma development

Debalina Mukhopadhyay[1], Balarko Chakraborty[1], Shreya Sarkar[1,3], Neyaz Alam[2] & Chinmay Kumar Panda[1]

Departments of [1]Oncogene Regulation & [2]Surgical Oncology, Chittaranjan National Cancer Institute, Kolkata, West Bengal, India & [3]New Brunswick Heart Centre, Saint John, NB, Canada

Received June 5, 2022

***Background & objectives*: Given the importance of the role of hypoxia induced pathway in different cancers including head-and-neck squamous cell carcinoma (HNSCC), this study delved into elucidating the molecular mechanism of hypoxia-inducible factor-1α (HIF1α) activation in HNSCC. Additionally, it analyzes the alterations of its regulatory genes [von Hippel–Lindau (*VHL*) and LIM domain containing 1 (*LIMD1)*] and target gene vascular endothelial growth factor (VEGF) in head-and-neck lesions at different clinical stages in relation with human papillomavirus (HPV) infection.**

***Methods*: Global mRNA expression profiles of HIF1α, *VHL, LIMD1* and VEGF were evaluated from public datasets of HNSCC, followed by validation of their expression (mRNA/protein) in an independent set of HPV+ve/–ve HNSCC samples of different clinical stages.**

***Results*: A diverse expression pattern of the HIF1α pathway genes was observed, irrespective of HPV infection, in the datasets. In validation in an independent set of HNSCC samples, high mRNA expressions of HIF1α/VEGF were observed particularly in HPV positive samples. However, *VHL/LIMD1* mRNA expression was low in tumours regardless of HPV infection status. In immunohistochemical analysis, high/medium (H/M) expression of HIF1α/VEGF was observed in basal/parabasal layers of normal epithelium, with significantly higher expression in tumours, especially in HPV-positive samples. Conversely, high cytoplasmic VHL expression in these layers gradually decreased with the progression of HNSCC, regardless of HPV infection. A similar trend was noted in *LIMD1* expression (nuclear/ cytoplasmic) during the disease development. The methylation pattern of *VHL* and *LIMD1* promoters in the basal/parabasal layers of normal epithelium correlated with their expression, exhibiting a gradual increase with the progression of HNSCC. The H/M expression of HIF1α/VEGF proteins and reduced VHL expression was associated with poor clinical outcomes.**

***Interpretation & conclusions*: The results of this study showed differential regulation of the *LIMD1-VHL*-HIF1α pathway in HPV positive and negative HNSCC samples, illustrating the molecular distinctiveness of these two groups.**

Key words Basal/parabasal layers - HIF1α regulation - HNSCC-head-and-neck - SCC-squamous cell carcinoma - HPV - normal oral epithelium - prognosis

© 2024 Indian Journal of Medical Research, published by Scientific Scholar for Director-General, Indian Council of Medical Research
This open access publication is protected under CC-BY-NC-SA 4.0

Head-and-neck squamous cell carcinoma (HNSCC) is one of the most common type of head and neck cancer worldwide and constitutes approximately one-third of all cancer cases from India[1]. Along with tobacco, differential human papillomavirus (HPV) [high risk(hr)-HPV 16/18] infection rate (0-86.6%), irrespective of anatomical sub-sites, has also been reported to be a major etiological factor[2-6]. It appears that recurrent exposure of stem cell-like cells in the basal/parabasal layers of normal oral epithelium to HPV infection or tobacco-associated carcinogens might promote alteration in the intracellular environment, such as oxidative stress response, leading to activation of hypoxia response pathway, which is directly involved in cancer development and progression[2,7-9]. The hypoxia response pathway is characterized by the stabilization of hypoxia-inducible factor1α (HIF1α) protein and vascular endothelial growth factor (VEGF) overexpression, plays a prominent oncogenic role in HNSCC development along with various other solid tumours[10,11]. Escalating over-expression of HIF1α (15-50%) has been noted during HNSCC progression, resulting in adverse prognosis[12]. Additionally, VEGF, responsible for angiogenesis, has been reported to be overexpressed in 90 per cent of the HNSCC samples, indicating its correlation with disease progression, chemoresistance and poor survival[13]. It is well reported that Von Hippel–Lindau *(VHL)* ubiquitinates HIF1α within the nucleus through its interaction with *LIMD1* as a bridging protein, followed by cytoplasmic transportation of the protein complex for HIF1α degradation that subsequently results in reduced expression of VEGF[11,14,15]. Frequent inactivation of *LIMD1* and *VHL* in different sets of HNSCC samples have been reported[16,17] along with *LIMD1* alterations (mutation, methylation/deletion), reduced mRNA and protein expression[18,19]. Similarly, loss of heterozygosity (52-67%) at chromosomal location 3p25, residing position of *VHL*, has been reported in HNSCC[20]. While null or low expression of *VHL* was noted in 63 per cent of the tongue cancer samples irrespective of *VHL* allelic alterations[17]. Therefore, HIF1α regulation is indisputably a crucial aspect linked to both the development as well as progression of HNSCC. In addition, HPV infection adds scope of alternative molecular features within HNSCC, resulting in heterogeneity within this tumour[21]. However, the role of the hr-HPV infection in the modulation of HIF1α regulation during HNSCC development has not yet been evaluated in detail.

This study focussed on investigating the comparative expression patterns of HIF1α pathway-associated and regulatory genes in different HNSCC datasets in association with or without HPV infection, followed by validation of the data at gene expression (RNA and protein) and epigenetic level in the independent HNSCC sample set of different clinical stages. It was found that HPV infection shows a distinct effect on the HIF1α regulation in HNSCC samples.

Material & Methods

This study was undertaken at the Department of Oncogene Regulation, Chittaranjan National Cancer Institute (CNCI), Kolkata after appropriate approval of the Institutional Ethical Committee and hospital authorities.

Sample collection: Freshly operated tumour tissues (n=62) and corresponding adjacent normal oral epithelium (n=58) were collected from 62 inpatients from the hospital section of CNCI, Kolkata. The collected tissues were divided to use for *(i)* immunohistochemical analysis by formalin fixation followed by paraffin embedding, *(ii)* RNA isolation and *(iii)* DNA isolation (Supplementary Fig. 1). Tumour grading and staging were done by two independent pathologists and clinicopathological information was collected.

Detection of human papillomavirus (HPV) 16 and 18: HPV infection was detected by polymerase chain reaction (PCR) technique, using MY09 and MY11 primers from the consensus L1 region of virus in the samples. HPV 16/18 typing analysis was done using type-specific primers from the E6 region of HPV 16 and the LCR region of HPV 18[22] (Supplementary Table I).

Quantitative analysis of mRNA expression: Total RNA was isolated from primary HNSCC tissue samples (n=30) and their adjacent normal oral tissues (n=30), using TRIzol reagent as manufacturer's instructions (Invitrogen, USA) (Supplementary Fig. 1). To perform reverse transcription for cDNA preparation, 1 μg of total RNA was used along with Random hexamer (Invitrogen, USA) and M-MuLV-Reverse Transcriptase (Promega, USA)[22]. Real-time PCR was done using SYBR Green Master Mix (Invitrogen, USA) as described earlier[22]. Fold expression change ($2^{-\Delta\Delta CT}$) was used to measure the relative expression of the genes against β2 microglobulin for normalization and

Table I. Demography of the patients with reference to human papillomavirus infection status

Features	n(%)	HPV 16		
		+ve, n(%)	–ve, n(%)	*P*
Total	62	30 (48)	32 (52)	
Age, mean±SD	52±13.37			
Mean≤	30 (50)	17 (57)	13 (43)	0.21
Mean>	32 (52)	13 (41)	19 (59)	
Gender				
Male	39 (63)	20 (51)	19 (49)	0.55
Female	23 (37)	10 (43)	13 (57)	
Primary site				
BM	28 (45)	9 (32)	19 (68)	0.077
TNG	10 (16)	5 (50)	5 (50)	
ALV	9 (15)	5 (56)	4 (44)	
Oropharynx	11 (18)	7 (64)	4 (36)	
Larynx	4 (6)	4 (100)	0 (0)	
TNM stage				
I	16 (26)	9 (56)	7 (44)	0.19
II	13 (21)	7 (54)	6 (46)	
III	17 (27)	10 (59)	7 (41)	
IV	16 (26)	4 (25)	12 (75)	
Grade				
Mild/WDSCC	39 (63)	23 (59)	16 (41)	0.09
Moderate/MDSCC	14 (23)	4 (29)	10 (71)	
Poor/PDSCC	9 (14)	3 (33)	6 (67)	
Node				
+ve	26 (42)	16 (62)	10 (38)	0.078
–ve	36 (58)	14 (39)	22 (61)	
Tobacco				
+ve	39 (63)	20 (51)	19 (49)	0.55
–ve	23 (37)	10 (43)	13 (57)	

P value represents level of significance during comparison. n, number of samples; BM, buccal mucosa; ALV, alveolus; TNG: tongue; WDSCC, well differentiated squamous cell carcinoma; MDSCC, moderately differentiated squamous cell carcinoma; PDSCC, poorly differentiated squamous cell carcinoma; –ve, factor absent; +ve, factor present; HPV, human papillomavirus; SD, standard deviation; TNM, tumour node metastasis

was plotted on a log scale[23], where ≥0.2 was considered as overexpression, ≤ - 0.2 as underexpression threshold and the range in between as no change (Supplementary Table I and II)

Protein expression analysis by immunohistochemistry: Protein expression of HIF1α, *VHL*, *LIMD1* and VEGF was studied by immunohistochemistry in the adjacent normal oral epithelium (n=58) and the corresponding HNSCC tissues (n=62) (Table I and Supplementary Fig. 1), which were sectioned at 5 µm thickness. The tissue sections (paraffin-embedded/cryosections) of HNSCC as well as the normal adjacent tissue were incubated overnight with primary antibodies against HIF1α (sc-53546), *VHL* (sc-5575), *LIMD1* (mouse monoclonal) and VEGF (sc-507) at a dilution of 1:100 at 4°C. Next, the HRP conjugated secondary antibodies, namely anti-mouse (sc-2005) and anti-rabbit (sc-2004) were used at 1:500 dilution each. 3, 3' diaminobenzidine (DAB) was used for chromogenic reaction and counterstained with haematoxylin. Slides were photographed under a Bright Field microscope (Leica DM1000, Germany) and evaluation was done according to method followed by Perrone *et al*[24], where

two independent observers grade the staining intensity as weak, moderate, or strong along with the percentage of positive cells. The final protein expression was reported as 0-2=low, 3- 5=intermediate, 6-7=high[24].

Microdissection and DNA extraction: *(i)* Microdissection of the malignant lesions was done for tumour region enrichment (>60%), using surgical knives under a dissecting microscope (Leica MZ16, Germany). The genomic DNA was isolated from the tissues as per routine protocol, described earlier[22]. The concentration of DNA was measured spectrophotometrically (Supplementary Fig. 1). *(ii)* The layer-wise promoter methylation analysis was done by using laser capture microscope (LCM, Palm microbeam, Zeiss, Germany) in normal oral epithelium, (n=30), following serial sectioning (paraffin/cryosections) and Haematoxylin-Eosin staining to identify basal/parabasal and spinous layers as described previously[22]. DNA was isolated from each layer according to the standard procedure[22]. (Supplementary Fig. 1).

Promoter methylation analysis: In order to study the epigenetic alterations, the promoter methylation analysis of *VHL* and *LIMD1* genes was performed in 30 composite oral epithelium samples, separated basal/parabasal (n=30) and spinous layer (n=30) from the same normal samples as mentioned above and corresponding HNSCC tumour tissues (n=30) as used in the RT-PCR analysis. The promoter methylation status was analyzed by PCR-based methylation-sensitive restriction analysis (MSRA). *Hpa*II (CCGG) restriction enzyme (Promega, Fitchburg, WI) was used to target the CpG-rich islands in the promoter regions of the genes[22]. The 445 bp fragment of the β-3A adaptin gene (K1) and the 229 bp fragment of RARβ2 (K2) served as controls for digestion and integrity, respectively[22] (Supplementary Table I and II).

Statistical analysis: To determine the risk associated with gene expression and other clinicopathological factors, Fisher's exact test was applied. All statistical tests used were 2-tailed and a significant level was considered at probability value, $P<0.05$. Kaplan–Meier method, followed by the Log-rank test, was used to plot survival curves. A multivariate Cox-proportional hazard regression model was used in order to test potential prognostic factors. Hazard ratio was then estimated for each potential prognostic factor with a 95 per cent confidence interval. All calculations were done using software Epi Info 7 (CDC, Atlanta) and IBM SPSS 23 (SPSS, Chicago, IL, USA).

Bioinformatics analysis: The differential mRNA expression pattern of the genes between HPV positive (HPV+ve) and HPV negative (HPV–ve) samples was data mined from HNCDB database[25] (*http://hncdb.cancerbio.info*). Five datasets: TCGA (HNSCC), GSE55542, GSE55544, GSE55546 and GSE39366 were used. The log fold change of the expression in HPV+ve samples with respect to HPV–ve samples was plotted on a heatmap for better visualization and understanding[25].

Results

Human papillomavirus (HPV) prevalence in the samples: The HPV infection was seen in 48 per cent (30/62) of the samples irrespective of clinical stages (Table I). Only HPV16 type was identified among the infected samples (Supplementary Fig. 2). Larynx (100%, 4/4) and oropharynx (64%, 7/11) subsites showed maximum infection rate, followed by alveolus (56%, 5/9), tongue (50%, 5/10) and buccal mucosa (32%, 9/28) subsites (Table I). HPV infection frequency was comparable between early-stage (stage I/II) (55%, 16/29) and late-stage (stage III/IV) (42%, 14/33) tumours (P=0.324) (Table I). In the case of tumour grade, node positivity and tobacco usage, HPV infection did not show any significant association (Table I).

Expression profile of the hypoxia-inducible factor-1α (HIF1α) pathway associated genes:

Different head-and-neck squamous cell carcinoma (HNSCC) datasets: The comprehensive data mining from the HNCDB database in HPV+ve and HPV–ve HNSCC samples showed a differential expression pattern of HIF1α (log fold change –0.8 to 0.11). Interestingly, significantly low HIF1α expression was noted in HPV+ve samples in three of the datasets (GSE55544, GSE55542 and TCGA) (Fig. 1, Supplementary Fig. 3A and Supplementary Table III). Similarly, significant low expression of *VHL* (log fold change: –0.07 to 1.55) and *LIMD1* (log fold change: –0.61 to –0.48) were evident in HPV+ve samples in three of the datasets (GSE55544, GSE55542, TCGA) and one dataset (GSE39366), respectively (Fig. 1, Supplementary Fig. 3B, C and Supplementary Table III). On the other hand, VEGF (log fold change: –0.19 to 0.33) showed significantly higher mRNA expression in HPV+ve samples in a single dataset (GSE55546)

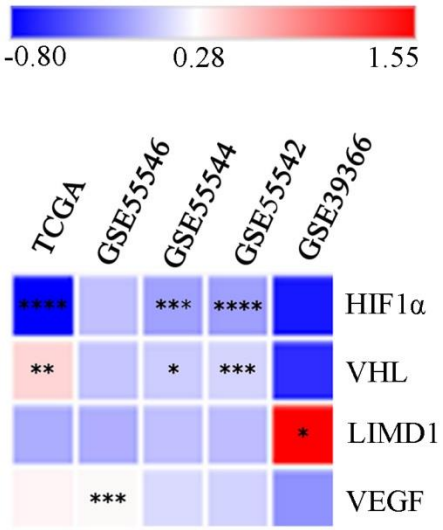

Fig. 1. Global mRNA expression profile of the HIF1α pathway associated genes in HPV+ve/–ve HNSCC samples. The heatmap showing log fold change of expression of the HIF1α pathway associated genes in HPV+ve samples in comparison to HPV–ve HNSCC samples (P^*<0.05, **<0.01, ***<0.001, ****<0.0001). HIF1α, hypoxia-inducible factor-1α; HPV, human papilloma virus; HNSCC, head and neck squamous cell carcinoma; VEGF, vascular endothelial growth factor; *VHL*, von Hippel–Lindau; *LIMD1*, LIM domain containing 1.

(Fig. 1, Supplementary Fig. 3D and Supplementary Table III).

Primary head-and-neck squamous cell carcinoma (HNSCC) samples: Of the HNSCC samples (n=30), overexpression of HIF1α and VEGF with 0.36 and 0.37 median log-fold changes was seen, respectively, with gradual increase with the advancement of the disease (Fig. 2A). However, reduced expression in *VHL* (-0.3 fold change) and *LIMD1* (-0.2 fold change) was noted in the samples with continuous downregulated expression with the disease progression (Fig. 2A). Interestingly, the expression of HIF1α was significantly higher in HPV+ve HNSCC than in the HPV–ve HNSCC samples (P=0.025); whereas *VHL* (P=0.182), *LIMD1* (P=0.083) and VEGF (P=0.493) expression was comparable in between HPV+ve and HPV–ve HNSCC samples (Fig. 2B and Supplementary Table IV).

Expression analysis of HIF1α/LIMD1/ VHL/ VEGF proteins in samples:

HIF1α expression profile: HIF1α showed distinct nuclear expression in the tissues. The basal/parabasal expression (43%, 25/58) was significantly higher

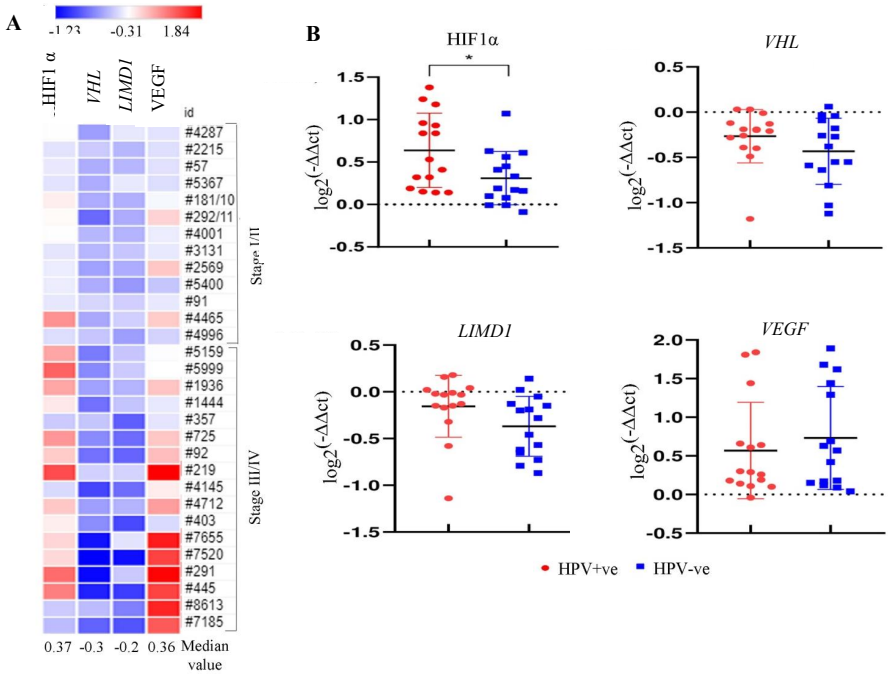

Fig. 2. mRNA expression pattern of HIF1α pathway genes in HNSCC primary tissue samples in comparison to adjacent normal tissue in correlation with HPV infection. (**A**) The heatmap representing the fold change expression of the genes in each tumour tissue sample in comparison to their paired adjacent normal according to the stage. The median fold change of each gene is also shown. (**B**) The dot plot representing the comparative analysis of mRNA expression of the HIF1α pathway genes (HIF1α, *VHL, LIMD1,* VEGF) in HPV+ve/–ve HNSCC samples (P^* <0.05).

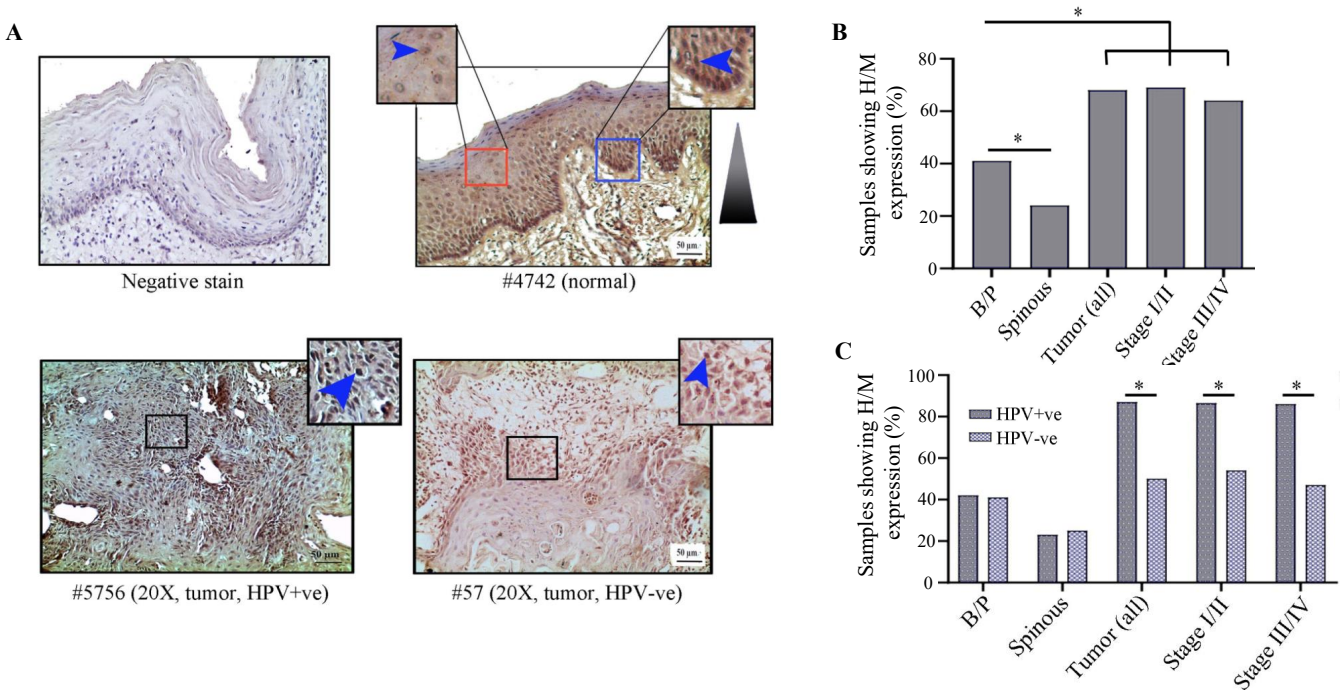

Fig. 3. Immunohistochemical analysis of HIFα protein in HPV+ve/–ve tumours and adjacent normal oral epithelium. (**A**) Representative image of expression pattern (nuclear) of HIF1α in different layers (B/P and spinous layers) of adjacent normal epithelium and HPV+ve/HPV–ve tumour tissue samples. Inset showing high-power view of the same. (**B**) The bar graph represents H/M expression of HIF1α in different layers of adjacent normal and tumour tissues of different clinical stages, irrespective of HPV infection status. (**C**) Bar graph represents HPV infection specific H/M expression pattern of HIF1α in different layers of adjacent normal and tumour tissues of different clinical stages. Blue arrows and blue gradient triangles indicate nuclear expression and nuclear expression pattern, respectively (P^*<0.05). B/P, basal/parabasal layers; H/M, high/medium.

than the spinous layer (24%, 14/58) (P=0.03) (Fig. 3A and B). The tumours showed substantially higher expression (68%, 42/62) than the basal/parabasal layers (P=0.006) (Fig. 3A, B and Supplementary Table V). Further, the distribution of tumours in early (stage I/II) and late (stage III/IV) stages demonstrated comparable high/medium (H/M) expression pattern in 72 per cent (21/29) and 64 per cent (21/33) of the samples, respectively (Fig. 3B).

The expression profile of HIF1α was comparable in both HPV+ve and HPV–ve basal/parabasal as well as spinous layers of the normal oral epithelium (Supplementary Table V), whereas HPV+ve tumour samples (87%, 26/30) showed significantly higher expression in comparison to the HPV–ve tumour samples (50%, 16/32) (P=0.002) (Fig. 3C and Supplementary Table V). A similar expression pattern was also noted with the progression of the disease in HPV+ve *vs.* HPV–ve samples, *i.e.* stage I/II (88% 14/16 *vs*. 54%, 7/13, P=0.045) and stage III/IV (86%, 12/14 *vs*. 47%, 9/19, P=0.023), respectively (Fig. 3C).

VHL expression profile: *VHL* showed differential subcellular expression patterns between basal/parabasal and the spinous layers of normal oral epithelium (Fig. 4A and B). It was noted that the proliferating basal/parabasal layers had predominant high/medium cytoplasmic expression (74%, 43/58) than the nuclear compartment (53%, 31/58) (Fig. 4A, B and Supplementary Table V). Contrastingly, cells in spinous layers showed prevalent high/medium nuclear expression (71%, 44/62) than the cytoplasmic subcellular location (55%, 34/62) (Fig. 4A, B and Supplementary Table V). The signature expression pattern of *VHL* in the basal/parabasal layers was noted in tumour samples but in significantly lower frequency with 44 per cent (27/62) cytoplasmic (P=0.0006) and 23 per cent (14/62) nuclear expression (P=0.0004) (Fig. 4A, B and Supplementary Table V). It was also noted that the nuclear expression (stage I/II: 21%, 6/29 and stage III/IV: 24%, 8/33) remained comparable (P=0.74), but the cytoplasmic expression (stage I/II: 55%, 16/29 and stage III/IV: 33%, 11/33, P=0.086) of *VHL* decreased with the progression of the disease (Fig. 4A and B).

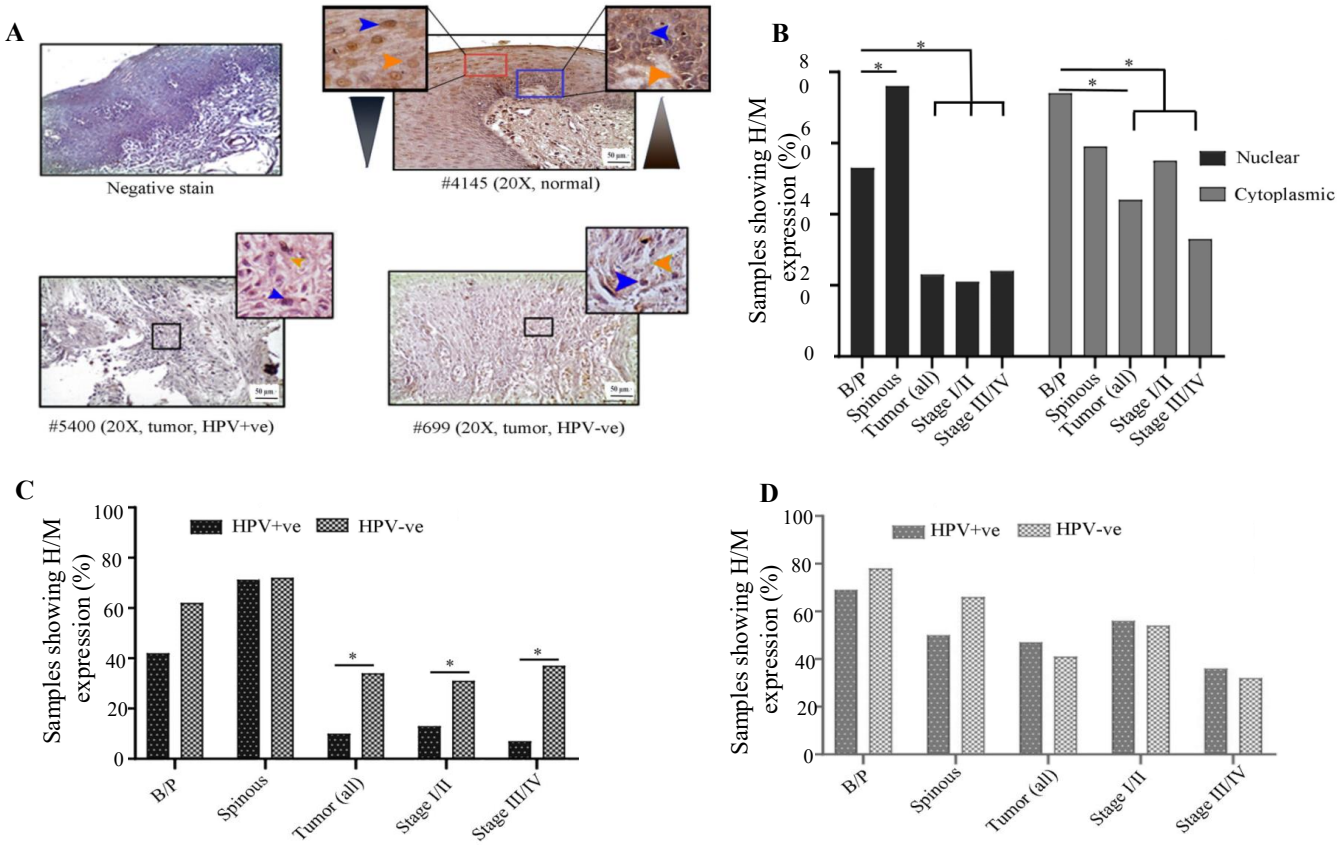

Fig. 4. Immunohistochemical analysis of *VHL* protein in HPV+ve/–ve tumours and adjacent normal oral epithelium. (**A**) Representative image of the expression pattern (nuclear/cytoplasmic) of *VHL* in different layers (B/P and spinous layers) of adjacent normal epithelium and HPV+ve/HPV–ve tumour tissue samples. The insets are showing high-power view of the respective image. (**B**) Bar graph represents H/M expression of *VHL* in nuclear and cytoplasmic compartments in different layers of adjacent normal and tumours tissues of different clinical stages, irrespective of HPV infection status. (**C and D)** The bar graphs represent HPV infection specific comparative expression pattern of *VHL* in nuclear and cytoplasmic compartments in different layers of adjacent normal and tumours tissues of different clinical stages. Blue and orange arrows indicate nuclear and cytoplasmic expression, respectively and grey gradient triangle indicates nuclear/cytoplasmic expression pattern (P^* <0.05).

HPV infection status-specific expression analysis showed that nuclear expression in both HPV+ve and HPV–ve basal/parabasal (HPV+ve: 42%, 11/26 and HPV–ve: 63%, 20/32; *P*=0.13) and spinous layers (HPV+ve: 70%, 21/26 and HPV–ve: 72%, 23/32; *P*=0.44) of normal oral epithelium were comparable (Fig. 4C and Supplementary Table V). Similarly, cytoplasmic expression of the basal/parabasal (HPV+ve: 69%, 18/26 and HPV–ve: 78%, 25/32; *P*=0.45) and spinous layers (HPV+ve: 50%, 13/26 and HPV–ve: 66%, 21/32; *P*=0.24) were also uniform in both the groups *i.e*. HPV+ve and HPV–ve (Fig. 4D and Supplementary Table V). In the case of tumour tissues, nuclear expression was significantly low in HPV+ve (10%, 3/30) than the HPV–ve samples (34%, 11/32) (*P*=0.022) in different clinical stages (Fig. 4C and Supplementary Table V). However, cytoplasmic expression of *VHL* was comparable between HPV+ve (47%, 14/30) and HPV–ve (41%, 13/32) tumour samples regardless of the progression of the disease (Fig. 4D and Supplementary Table V).

LIMD1 expression profile: In normal oral epithelium uniform nuclear (both basal/parabasal and spinous: 78%, 45/58) and cytoplasmic (basal/parabasal: 62%, 36/58; spinous: 60%, 35/58), the expression of *LIMD1* was noted (Fig. 5A, B and Supplementary Table V). In tumours, only 55 per cent (34/62) of the samples showed high/medium nuclear expression, which was significantly low in comparison to basal/parabasal layers (*P*=0.0084) (Fig. 5A, B and Supplementary Table V). Stage-specific distribution showed comparable high/medium nuclear expression (stage I/II: 59%, 17/29 and stage III/IV: 52%, 17/33; *P*=0.58) (Fig. 5B). Similarly, only 31 per cent (19/62) of the tumours showed high/medium cytoplasmic expression,

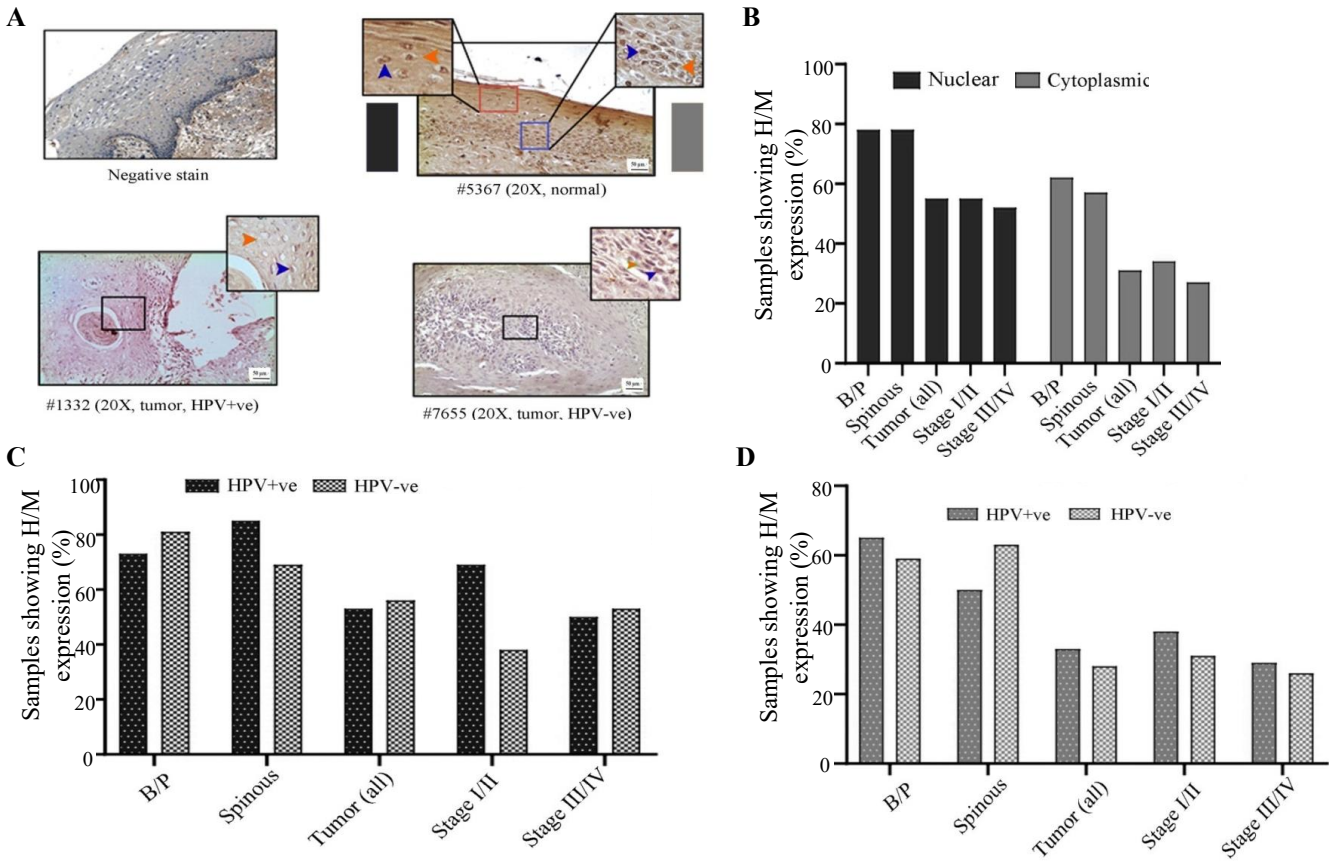

Fig. 5. Immunohistochemical analysis of *LIMD1* protein in HPV+ve/–ve tumours and adjacent normal oral epithelium. (**A**) Representative image of the expression pattern (nuclear/cytoplasmic) of *LIMD1* in different layers (B/P and spinous layers) of adjacent normal epithelium and HPV+ve/HPV–ve tumour tissue samples. The insets are showing high-power view of the respective image. (**B**) The bar graph represents H/M expression of *LIMD1* in nuclear and cytoplasmic compartments in different layers of adjacent normal and tumours tissues of different clinical stages, irrespective of HPV infection status. (**C** and **D**) The bar graphs represent HPV infection specific comparative expression pattern of *LIMD1* in nuclear and cytoplasmic compartments in different layers of adjacent normal and tumours tissues of different clinical stages. Blue and orange arrows indicates nuclear and cytoplasmic expression, respectively and grey gradient rectangle indicates nuclear/cytoplasmic expression pattern.

which was considerably lower than the cytoplasmic expression of basal/parabasal layers (P=0.018) and the expression pattern also gradually decreased with the progression of the disease (stage I/II: 34%, 10/29 and stage III/IV: 27%, 9/33; P=0.55) (Fig. 5A and B).

The expression pattern depending on HPV infection status showed that nuclear expression in basal/parabasal (HPV+ve: 73%, 19/26 and HPV–ve: 81%, 26/32; P=0.47) and spinous layers (HPV+ve: 85%, 22/26 and HPV–ve: 72%, 23/32; P=0.17) of normal oral epithelium were comparable (Fig. 5C, D and Supplementary Table V). Similar result was obtained for the cytoplasmic expression of *LIMD1* in basal/parabasal (HPV+ve: 65%, 17/26 and HPV–ve: 59%, 19/32; P=0.65) and spinous layers (HPV+ve: 50%, 13/26 and HPV–ve: 69%, 22/32; P=0.35) (Fig. 5C, D and Supplementary Table V). The nuclear (HPV+ve: 53%, 16/30 and HPV–ve: 56%, 18/32; P=0.82) and cytoplasmic (HPV+ve: 33%, 10/30 and HPV–ve: 28%, 9/32; P=0.66) expression of *LIMD1* was also found to be comparable in both HPV+ve and HPV–ve tumour samples (Fig. 5C, D and Supplementary Table V), even when the tumours were distributed according to the stage (stage I/II and stage III/IV) (Fig. 5C and D).

VEGF expression profile: VEGF expression was restricted in cytoplasm in both normal oral epithelium and tumours. It was noted that 43 per cent (25/58) and 24 per cent (14/58) of the samples showed high/medium cytoplasmic expression in basal/parabasal and spinous layers in normal oral epithelium, respectively

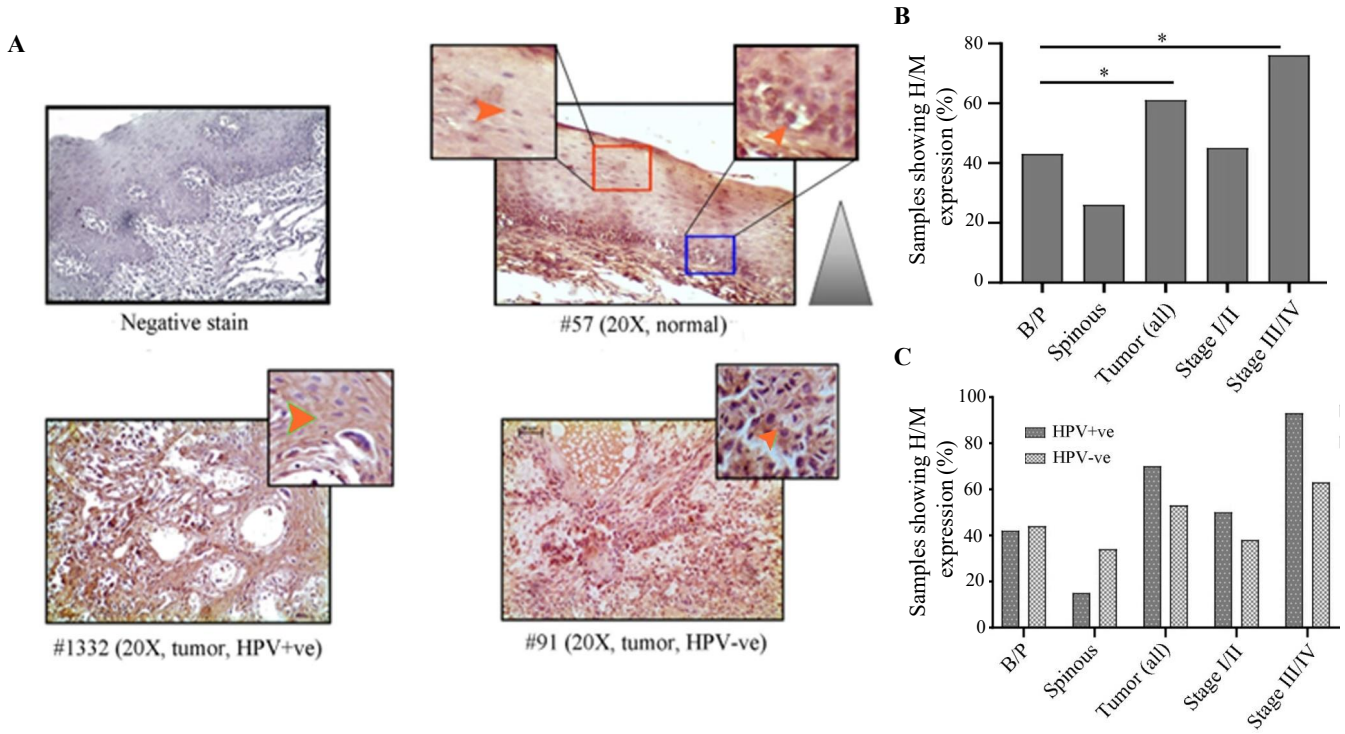

Fig. 6. Immunohistochemical analysis of VEGF protein in HPV+ve/–ve tumours and adjacent normal oral epithelium. (**A**) Representative image of expression pattern (cytoplasmic) of VEGF in different layers (B/P and spinous layers) of adjacent normal epithelium and HPV+ve/HPV–ve tumour tissue samples. The insets are showing high-power view of the respective image. (**B**) The bar graph represents H/M expression of VEGF in different layers of adjacent normal and tumour tissues of different clinical stages, irrespective of HPV infection status. (**C**) The bar graph represents HPV infection specific H/M expression pattern of VEGF in different layers of adjacent normal and tumour tissues of different clinical stages. Orange arrows indicate cytoplasmic expression and grey gradient triangle indicates cytoplasmic expression pattern (P^* <0.05).

(*P*=0.051) (Fig. 6A, B and Supplementary Table V). However, 61 per cent (38/62) of the samples showed high/medium cytoplasmic expression in tumours, which was significantly different from basal/parabasal layers (*P*=0.04) (Fig. 6A, B and Supplementary Table V). The stage-specific distribution showed 45 per cent (13/29) and 76 per cent (25/33) high/medium expression in stage I/II and stage III/IV tumour samples, respectively (*P*=0.012) (Fig. 6B).

It was found that HPV+/–ve basal/parabasal (HPV+ve: 42%, 11/26 HPV–ve: 44%, 14/32; *P*=0.91) and spinous (HPV+ve: 15%, 4/26 HPV–ve: 34%, 11/32; *P*=0.1) layers of oral epithelium showed comparable cytoplasmic expression (Fig. 6C and Supplementary Table V). In the case of tumours, 70 per cent (21/30) of the HPV+ve samples and 53 per cent (17/32) of the HPV–ve samples showed high/medium VEGF expression (Fig. 6C and Supplementary Table V). However, the difference in the expression pattern between HPV+ve and HPV–ve groups was not significant (*P*=0.18). However, the expression pattern was distinctly different between HPV+ve (93%, 13/14) and HPV–ve (63%, 12/19) tumours in late-stage (stage III/IV) (*P*=0.051) than the early-stage (stage I/II) tumours (HPV+ve: 50%, 8/16; HPV–ve: 38%, 5/13; *P*=0.55) (Fig. 6C).

Association between HIF1α, LIMD1, VHL and VEGF proteins based on expression: It was found that high HIF1α protein expression in the nucleus was significantly correlated with reduced nuclear expression of *VHL* (r=-0.45, *P*=0.002) and high expression of VEGF (r=0.037, *P*=0.003) in tumour samples. However, no such association was noted between the nuclear expression of HIF1α and *LIMD1* (r=0.072, *P*=0.58) in the tumour tissues (Supplementary Fig. 4).

Methylation status of VHL and LIMD1 genes in the samples: In normal oral epithelium, the overall methylation frequency of *VHL* was seen in 17 per cent (5/30) of the samples (Fig. 7Ai and ii) with a gradual

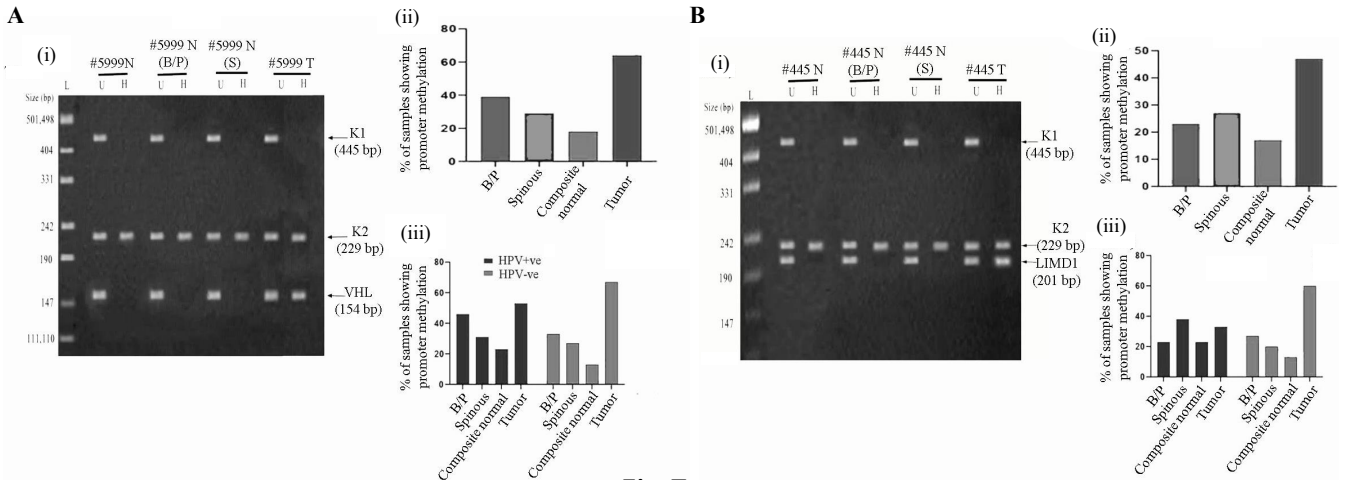

Fig. 7. Promoter methylation analysis of *VHL* and *LIMD1* genes in HPV+ve and HPV–ve samples. (**A & B**); Panels **(i)** Representative gel image of promoter methylation analysis using MSRA method for B/P and spinous layers, whole normal (composite) and its corresponding tumour samples. (**ii**) The bar graph represents the methylation frequency of the genes in different layers of normal oral epithelium, composite normal and corresponding HNSCC tissue samples irrespective of their HPV infection status. (**iii**) The bar graph represents HPV infection specific methylation frequencies of the genes in the same set of samples. U, undigested samples; H, Hpa*II* digested samples.

decrease from basal/parabasal (39%, 11/28) to spinous layers (29%, 8/28) (Fig. 7Ai and ii). Like the basal/parabasal layers, high methylation in *VHL* (60%, 18/30) was seen in the tumours (*P*=0.12) (Fig. 7Ai and ii). However, the promoter methylation pattern of *VHL* was comparable in basal/parabasal, spinous and composite normal samples irrespective of HPV infection (Fig. 7A-iii). Similarly, comparable methylation frequencies were also noted in HPV+ve (53%, 8/15) and HPV–ve (67%, 10/15) tumours (*P*=0.47) (Fig. 7Aiii).

In normal oral epithelium, 18 per cent, (5/28) of the samples showed *LIMD1* methylation, followed by comparable frequencies of methylation in basal/parabasal (25%, 7/28) and spinous layers (29%, 8/28) (Fig. 7Bi and ii). However, high promoter methylation of *LIMD1* (47%, 14/30) was seen in the tumours in comparison to the basal/parabasal layers (*P*=0.089) (Fig. 7Bi and ii).

In HPV+ve/–ve normal oral epithelium, methylation frequency of *LIMD1* did not change significantly (HPV+ve: 23%, 3/13; HPV–ve: 13%, 2/15; *P*=0.52) (Fig. 7Biii). Similar methylation frequency was also seen in HPV+ve/–ve basal/parabasal (HPV+ve: 23%, 3/13; HPV–ve: 27%, 4/15; *P*=0.83) and spinous (HPV+ve: 39%, 5/13; HPV–ve: 20%, 3/15; *P*=0.3) layers (Fig. 7Biii). Interestingly, high promoter methylation of *LIMD1* was seen in HPV–ve tumour (60%, 9/15) than HPV+ve samples (33%, 5/15), but was not significant (*P*=0.15) (Fig. 7Biii).

Clinico-pathological correlation of gene alterations: It was noted that tumour stage was the common potential risk factor associated with disease development as found in both univariate and multivariate analysis (Table II). However, tumour grade and lymph node positivity were found to be potential risk factors only in univariate regression analysis (Table II). HIF1α and *VHL* expression patterns (nuclear and cytoplasmic) were found to be the prominent risk factors in both univariate and multivariate regression analysis (Table II), whereas VEGF expression was found to be one of the risk factors as per univariate analysis alone (Table II).

In survival analysis, high/medium nuclear expression of HIF1α protein, low nuclear/cytoplasmic expression VHL protein expression and high/medium cytoplasmic VEGF expression showed significantly worse prognosis among the HNSCC groups (Supplementary Fig. 5A-C and F). No such association was seen in *LIMD1* (nuclear/cytoplasmic) protein expression (Supplementary Fig. 5D and E). Interestingly, high/medium co-expression of HIF1α and VEGF showed poor clinical outcomes (Supplementary Fig. 6A). Moreover, co-alteration in *VHL* and *LIMD1* expression (low nuclear/cytoplasmic) was associated with worst prognosis among the patients (Supplementary Fig. 6B and C).

Discussion

Different studies have reported the clinical significance of HPV infection in HNSCC development

Table II. Regression analysis showing the association between potential risk factors and survival rate

Variables	Significant	Exp(B)	95.0% CI for Exp(B)	
			Lower	Upper
A. Univariate Cox regression analysis				
Stage	0.002	0.418	0.243	0.717
HPV infection	0.222	1.398	0.817	2.391
Tobacco usage	0.464	0.817	0.476	1.404
Lymph node	0	2.783	1.608	4.816
Grade	0.048	1.447	1.004	2.086
HIF1α nuclear expression	0	3.154	1.694	5.873
VHL nuclear expression	0	0.119	0.048	0.294
VHL cytoplasmic expression	0	0.176	0.095	0.328
LIMD1 nuclear expression	0.643	0.882	0	1.502
LIMD1 cytoplasmic expression	0.165	0.657	0.364	1.189
VEGF cytoplasmic expression	0	3.657	2.036	6.568
B. Multivariate Cox regression analysis				
Stage	0	0.126	0.049	0.329
HPV infection	0.378	0.733	0.367	1.462
Tobacco usage	0.241	1.566	0.739	3.316
Lymph node	0.554	1.333	0.514	3.461
Grade	0.767	1.079	0.653	1.783
HIF1α nuclear expression	0	6.231	2.437	15.928
VHL nuclear expression	0	0.062	0.018	0.217
VHL cytoplasmic expression	0.001	0.204	0.083	0.501
LIMD1 nuclear expression	0.784	0.906	0.448	1.832
LIMD1 cytoplasmic expression	0.422	1.397	0.618	3.158
VEGF cytoplasmic expression	0.774	1.116	0.528	2.356

Cox proportional hazard regression model to determine prognostic importance of protein expression alterations and different clinico-pathological parameters in patients. B, hazard ratio; CI, confidence interval; HIF1α, hypoxia-inducible factor-1α; VEGF, vascular endothelial growth factor; *VHL*, von Hippel–Lindau

as well as progression[2-6].This was also reflected in the present study where the collected samples showed 48 per cent HPV infection frequency with 100 per cent HPV16 infection prevalence.

In the comprehensive data mining approach, it was noted that the genes associated with the HIF1α pathway have differential expression patterns in both HPV+/–ve HNSCC samples. Lower expression patterns of HIF1α and *VHL* were noted in HPV+ve HNSCC samples in three datasets (GSE55544, GSE55542, TCGA), whereas in majority (4/5) of the datasets, *LIMD1* and VEGF showed comparable expression patterns in HPV+/–ve HNSCC samples, indicating that HPV infection might have some role in regulating some of these genes. The bioinformatics data was validated in the collected HNSCC samples, revealing elevated HIF1α and *VEGF* mRNA expression with disease progression, thereby confirming their oncogenic role[11-13]. In accordance with the mRNA expression pattern in the primary HNSCC samples, significantly high HIF1α (nuclear) and VEGF (cytoplasmic) protein expressions were noted in the tumour tissues, which increased parallels with the disease progression similar to prior reports[11-13]. In the normal oral epithelium, significantly high HIF1α and VEGF protein expressions were noted in basal/parabasal layers in comparison to the spinous layers, confirming their proactive role in cell proliferation[26].

Similar to the mRNA expression, the HIF1α protein expression was significantly higher in HPV+ve

than HPV–ve tumours[9] and VEGF protein also showed a similar trend. Several studies have suggested that HPV perturb the redox balance[27] in the host cell for the viral life cycle and viral DNA integration into the host's genome[28] and thereby activate redox-sensitive pathways resulting in high transcription rate and subsequently high protein expression/stabilization of VEGF and HIF1α in HPV+ve tumour tissues[9,29,30]. However, comparable HIF1α expression has also been reported in HNSCC, irrespective of HPV infection, opposing the interpretation of the direct association between HIF1α/VEGF and HPV infection in head-and-neck malignancy[31,32]. Although the HIF1α/VEGF transcription/translation rate was lower in HPV–ve HNSCC samples than in HPV+ve tumour tissues, it remained higher than in normal epithelium. This could be attributed to the intrinsic cellular response to hypoxia induced in solid tumour[33].

Contrastingly, *LIMD1* and *VHL* tumour suppressive role was authenticated with a gradual decrease in mRNA expression in advanced tumour stages. These mRNA data were further validated by the protein expression, showing lower expression of both VHL and LIMD1 protein in the tumour tissues[16,17]. It was interesting to note that VHL protein showed preferential cytoplasmic expression in basal/parabasal than the spinous layers of normal oral epithelium and also in tumour tissues. Previously it was reported that VHL remains sequestered in cytoplasm in proliferating cells as it interferes with the assembly of transcriptionally active Elongin complexes and displaces Elongin A, inhibiting the transcription of the cell proliferation associated genes[34,35]. This might be the reason for the differential nucleo-cytoplasmic localization of VHL in proliferating basal/parabasal layers and non-proliferating mature spinous layers of normal oral epithelium and also in the tumour tissues[34-37]. However, both the nuclear and the cytoplasmic expression of VHL gradually reduced in tumour tissues with the progression of the disease, indicating its overall tumour suppressive role during HNSCC development[38-40].

The *VHL* and *LIMD1* mRNA expression was comparable in both HPV+ve and HPV–ve tumour samples. When we classified the protein expression pattern of *VHL* in normal epithelium in association with HPV infection, it was found that *VHL* nucleo-cytoplasmic expression was similar in both the layers of normal epithelium irrespective of HPV infection status, confirming insignificant influence of HPV on *VHL* expression in normal tissues. Interestingly, in tumour tissues, the nuclear expression was found to be significantly lower in the HPV+ve group than HPV–ve, especially in the advanced stages. However, this statement needs to be authorized by further studies. Studies have reported that viruses exploit the host's ubiquitinoylation machinery and reprogramme the substrate specificity, leading to cellular transformation[41,42]. It was documented that HPV oncoprotein E7 replaces *VHL* from the E3 ubiquitin ligase complex and heavily ubiquitinates *VHL* itself, reducing its nuclear localization and stability in HPV+ve tumour tissues, resulting in high HIF1α and VEGF expression[43-45]. However, this statement needs further verification by confirming protein-protein interaction by co-immunoprecipitation in both HPV+ve and HPV–ve cell lines. In the HPV–ve tumour tissue, low *VHL* expression (nuclear/cytoplasmic) was also noted, which could be explained by frequent genetic/epigenetic alteration of *VHL* in HNSCC as reported by several other studies[17,20]. The *LIMD1* protein showed relative expression in both HPV+ve and HPV–ve tumour samples, corroborating its HPV infection-independent downregulated expression during disease development[18,19].

It is important to mention that discrepancies in the mRNA expression pattern of genes between some of the datasets and our HNSCC samples might be due to differences in the methodology used in the analysis and etiological factors associated with the disease.

The oncogenic role of HIF1α showed a significant positive association with VEGF in HNSCC tissues like other cancers[46,47]. Therefore, assessment of the HIF1α and VEGF co-operative expression pattern in malignant samples could be used as predictive markers to analyze the tumour behaviour, important for selecting suitable targeted therapy[48-50]. However, a report is also available pointing to no significant association between these two proteins in oral squamous cell carcinoma[51]. The agnostic role of *VHL* against HIF1α was validated by their significant negative correlation in the primary HNSCC tissue samples, conceivably indicating potentiality of *VHL* as therapeutic candidate. Alternatively, the insignificant association of HIF1α with *LIMD1* was noted in HNSCC samples, implying *LIMD1* independent HIF1α regulation[52] while, several studies have also validated the crucial role of *LIMD1* in HIF1α stabilization[53].

The promoter methylation pattern of *VHL* and *LIMD1* was consistent with their mRNA/protein

expression data, indicating methylation as one of the molecular mechanisms for the *VHL* and *LIMD1* reduced expression in tumour tissues[19]. The *VHL* showed comparable methylation frequency in both HPV+ve and HPV–ve tumour tissues, but the methylation percentage of *LIMD1* was higher in HPV–ve as compared to HPV+ve tumours. Although the difference in methylation frequency between HPV+ve and HPV–ve samples was not significant, it suggested a trend among samples with a probable distinct molecular event for *LIMD1* in HPV–ve tumour. It is noteworthy that several studies have also reported allelic deletion along with methylation in both *VHL* and *LIMD1* in HNSCC samples resulting in their lower expression in tumour tissues[16-20]. We also did the layer-wise methylation analysis for both *VHL* and *LIMD1* in normal oral epithelium, but no significant difference was noted, even in the presence or absence of HPV infection.

Finally, the risk analysis and survivability study showed that tumour stage, HIF1α, VEGF and *VHL* expression patterns in different subcellular pockets play an imperative role in HNSCC, indicating their potentiality as the key regulatory factors. It is important to highlight that high/medium expression of HIF1α and its target gene VEGF are associated with poor patient prognosis as these might contribute to tumour metastasis and further aggressiveness of the disease. While under expression of *VHL* in both nuclear and cytoplasmic locations facilitate HIF1α stability and might be responsible for poor patient outcomes. These data were further validated with the poor patient survivability in tumour samples showing high/medium co-expression of HIF1α–VEGF or low co-expression of *VHL-LIMD1* (nuclear/cytoplasmic).

Several HIF1α, VEGF and *VHL* targetable therapeutic molecules have been under clinical trial for HNSCC treatment, but none has so far received a concession for clinical use in HNSCC patients. This study features the distinct molecular profile of HIF1α and its associated/regulatory genes in HNSCC; moreover, it also focuses on the comparative discrete expression pattern of these genes in HPV+ve and HPV–ve HNSCC among Indians. This study offers information related to prognosis and clinical strategies to opt for combinatorial therapeutic intervention along with the existing strategies depending on the HPV-specific disease condition.

***Acknowledgment*:** The authors acknowledge the receipt of primary antibody –*LIMD1*(mouse monoclonal) as a gift from Dr. Tyson V. Sharp, Barts Cancer Institute, Queen Mary University of London.

***Financial support & sponsorship*:** This study received financial support from Department of Science and Technology (Govt. of India), Kiran Division (SR/WOS-A/LS-278/2016). Author BC received UGC-NET Fellowship (Sr. No. 2121430433, Ref. No.: 21/12 / 2014) & EU-V dated 08.06.2015. Author CKP received NASI Senior Scientist Platinum Jubilee Fellowship (2020).

***Conflicts of Interest*:** None.

Use of Artificial Intelligence (AI)-Assisted Technology for manuscript preparation: The authors confirm that there was no use of AI-assisted technology for assisting in the writing of the manuscript and no images were manipulated using AI.

References

1. Sharma J, Baishya N, Kataki A, Kalita C, Das A, Rahman T. Head and neck squamous cell carcinoma in young adults: A hospital-based study. *Indian J Med Paediatr Oncol* 2019; *40* : 18-22.
2. Murthy V, Calcuttawala A, Chadha K, d'Cruz A, Krishnamurthy A, Mallick I, *et al*. Human papillomavirus in head and neck cancer in India: Current status and consensus recommendations. *South Asian J Cancer* 2017; *6* : 93-8.
3. Balaram P, Nalinakumari KR, Abraham E, Balan A, Hareendran NK, Bernard HU, *et al*. Human papillomaviruses in 91 oral cancers from Indian betel quid chewers-high prevalence and multiplicity of infections. *Int J Cancer* 1995; *61* : 450-4.
4. Koppikar P, deVilliers EM, Mulherkar R. Identification of human papillomaviruses in tumors of the oral cavity in an Indian community. *Int J Cancer* 2005; *113* : 946-50.
5. Patel KR, Vajaria BN, Begum R, Desai A, Patel JB, Shah FD, *et al*. Prevalence of high-risk human papillomavirus type 16 and 18 in oral and cervical cancers in population from Gujarat, West India. *J Oral Pathol Med* 2014; *43* : 293-7.
6. Nandi S, Mandal A, Chhebbi M. The prevalence and clinicopathological correlation of human papillomavirus in head and neck squamous cell carcinoma in India: A systematic review article. *Cancer Treat Res Commun* 2021; *26* : 100301.
7. García-Guede Á, Vera O, Ibáñez-de-Caceres I. When Oxidative Stress Meets Epigenetics: Implications in Cancer Development. *Antioxidants (Basel)* 2020; *9* : 468.
8. Hielscher A, Gerecht S. Hypoxia and free radicals: role in tumor progression and the use of engineering-based platforms to address these relationships. *Free radi biol med* 2015; *79* : 281-91.
9. De Marco F. Oxidative stress and HPV carcinogenesis. *Viruses* 2013; *5* : 708-31.

10. Masoud GN, Li W. HIF-1α pathway: role, regulation and intervention for cancer therapy. *Acta Pharm Sin B* 2015; *5* : 378-89.
11. Johnson DE, Burtness B, Leemans CR, Lui VWY, Bauman JE, Grandis JR. Head and neck squamous cell carcinoma. *Nat Rev Dis Primers* 2020; *6* : 92.
12. Kurokawa T, Miyamoto M, Kato K, Cho Y, Kawarada Y, Hida Y, *et al*. Overexpression of hypoxia-inducible-factor 1α(HIF-1α) in oesophageal squamous cell carcinoma correlates with lymph node metastasis and pathologic stage. *Bri J cancer* 2003; *89* : 1042-7.
13. Micaily I, Johnson J, Argiris A. An update on angiogenesis targeting in head and neck squamous cell carcinoma. *Cancers Head Neck* 2020; *5* : 5.
14. Groulx I, Lee S. Oxygen-dependent ubiquitination and degradation of hypoxia-inducible factor requires nuclear-cytoplasmic trafficking of the von Hippel-Lindau tumor suppressor protein. *Mol Cell Biol* 2002; *22* : 5319-36.
15. Foxler DE, Bridge KS, James V, Webb TM, Mee M, Wong SC, *et al*. The LIMD1 protein bridges an association between the prolyl hydroxylases and VHL to repress HIF-1 activity. *Nat Cell Biol* 2012; *14* : 201-8.
16. Yoo WJ, Cho SH, Lee YS, Park GS, Kim MS, Kim BK, *et al*. Loss of heterozygosity on chromosomes 3p,8p,9p and 17p in the progression of squamous cell carcinoma of the larynx. *J Korean med sci* 2004; *19* : 345-51.
17. Hasegawa H, Kusumi Y, Asakawa T, Maeda M, Oinuma T, Furusaka T, *et al*. Expression of von Hippel-Lindau tumor suppressor protein (pVHL) characteristic of tongue cancer and proliferative lesions in tongue epithelium. *BMC cancer* 2017; *17* : 381.
18. Ghosh S, Ghosh A, Maiti GP, Mukherjee N, Dutta S, Roy A, *et al*. LIMD1 is more frequently altered than RB1 in head and neck squamous cell carcinoma: clinical and prognostic implications. *Mol cancer* 2010; *9* : 58.
19. Sarkar S, Alam N, Mandal SS, Chatterjee K, Ghosh S, Roychoudhury S, *et al*. Differential transmission of the molecular signature of RBSP3, LIMD1 and CDC25A in basal/parabasal versus spinous of normal epithelium during head and neck tumorigenesis: A mechanistic study. *PLoS One* 2018; *13* : e0195937.
20. Li X, Lee NK, Ye YW, Waber PG, Schweitzer C, Cheng QC, *et al*. Allelic loss at chromosomes 3p, 8p, 13q, and 17p associated with poor prognosis in head and neck cancer. *J Natl Cancer Inst* 1994; *86* : 1524-9.
21. Qin T, Li S, Henry LE, Liu S, Sartor MA. Molecular Tumor Subtypes of HPV-Positive Head and Neck Cancers: Biological Characteristics and Implications for Clinical Outcomes. Cancers. *Basel* 2021; 13 : 2721.
22. Chakraborty B, Mukhopadhyay D, Roychowdhury A, Basu M, Alam N, Chatterjee K, *et al*. Differential Wnt-β- catenin pathway activation in HPV positive and negative oral epithelium is transmitted during head and neck tumorigenesis: clinical implications. *Med Microbiol Immunol* 2021; *210* : 49-63.
23. Livak KJ, Schmittgen TD. Analysis of Relative Gene Expression Data Using Real-Time Quantitative PCR and the 2−ΔΔCT Method. *Methods* 2001; *25* : 402-8.
24. Perrone F, Suardi S, Pastore E, Casieri P, Orsenigo M, Caramuta S, *et al*. Molecular and Cytogenetic Subgroups of Oropharyngeal Squamous Cell Carcinoma. *Clin Cancer Res* 2006; *12* : 6643-51.
25. Zhang Q, Li X, Su X, Zhang H, Wang H, Yin S, *et al*. HNCDB: An Integrated Gene and Drug Database for Head and Neck Cancer. *Front Oncol* 2019; *9* : 371.
26. Chakraborty C, Mitra S, Roychowdhury A, Samadder S, Dutta S, Roy A, *et al*. Deregulation of LIMD1-VHL-HIF-1α-VEGF pathway is associated with different stages of cervical cancer. *Biochem J* 2018; *475* : 1793-806.
27. De Marco F. Oxidative stress and HPV carcinogenesis. *Viruses* 2013; *5* : 708-31.
28. Cruz-Gregorio A, Manzo-Merino J, Lizano M. Cellular redox, cancer and human papillomavirus. *Virus Res* 2018; *246* : 35-45.
29. Knuth J, Sharma SJ, Würdemann N, Holler C, Garvalov BK, Acker T, *et al*. Hypoxia-inducible factor-1α activation in HPV-positive head and neck squamous cell carcinoma cell lines. *Oncotarget* 2017; *8* : 89681-91.
30. Cruz-Gregorio A, Aranda-Rivera AK. Redox-sensitive signalling pathways regulated by human papillomavirus in HPV-related cancers. *Rev Med Virol* 2021; *31* : e2230.
31. Hong A, Zhang M, Veillard AS, Jahanbani J, Lee CS, Jones D, *et al*. The prognostic significance of hypoxia inducing factor 1-α in oropharyngeal cancer in relation to human papillomavirus status. *Oral Oncol* 2013; *49* : 354-9.
32. Göttgens EL, Ostheimer C, Span PN, Bussink J, Hammond EM. HPV, hypoxia and radiation response in head and neck cancer. *Br J Radiol* 2019; *92* : 20180047.
33. Beasley N, Leek R, Alam M, Turley H, Cox G, Gatter K, *et al*. Hypoxia-inducible factors HIF-1alpha and HIF-2alpha in head and neck cancer: relationship to tumor biology and treatment outcome in surgically resected patients. *Cancer Res* 2002; *62* : 2493-7.
34. Ye Y, Vasavada S, Kuzmin I, Stackhouse T, Zbar B, Williams BR. Subcellular localization of the von Hippel-Lindau disease gene product is cell cycle-dependent. *Int J Cancer* 1998; *78* : 62-9.
35. Lee S, Chen DY, Humphrey JS, Gnarra JR, Linehan WM, Klausner RD. Nuclear/cytoplasmic localization of the von Hippel-Lindau tumor suppressor gene product is determined by cell density. *Pro Nat Acad Sci USA* 1996; *93* : 1770-5.
36. Schoenfeld AR, Davidowitz EJ, Burk RD. Endoplasmic reticulum/cytosolic localization of von Hippel-Lindau gene products is mediated by a 64-amino acid region. *Int J Cancer* 2001; *91* : 457-67.
37. Lewis MD, Roberts BJ. Role of nuclear and cytoplasmic localization in the tumour-suppressor activity of the von Hippel-Lindau protein. *Oncogene* 2003; *22* : 3992-7.

38. Lonergan KM, Iliopoulos O, Ohh M, Kamura T, Conaway RC, Conaway JW, *et al*. Regulation of hypoxia-inducible mRNAs by the von Hippel-Lindau tumor suppressor protein requires binding to complexes containing elongins B/C and Cul2. *Mol Cell Biol* 1998; *18* : 732-41.
39. Lee S, Neumann M, Stearman R, Stauber R, Pause A, Pavlakis GN, *et al*. Transcription-dependent nuclear-cytoplasmic trafficking is required for the function of the von Hippel-Lindau tumor suppressor protein. *Mol Cell Biol* 1999; *19* : 1486-97.
40. Boedeker CC, Erlic Z, Richard S, Kontny U, Gimenez-Roqueplo AP, Cascon A, *et al*. Head and neck paragangliomas in von Hippel-Lindau disease and multiple endocrine neoplasia type 2. *J Clin Endocrinol Metab* 2009; *94* : 1938-44.
41. Gustin J, Moses A, Früh K, Douglas J. Viral Takeover of the Host Ubiquitin System. *Front Microbiol* 2011; *2* : 161.
42. Isaacson MK, Ploegh HL. Ubiquitination, ubiquitin-like modifiers, and deubiquitination in viral infection. *Cell Host & Microbe* 2009; *5* : 559-70.
43. Huh K, Zhou X, Hayakawa H, Cho JY, Libermann TA, Jin J, *et al*. Human papillomavirus type 16 E7 oncoprotein associates with the cullin 2 ubiquitin ligase complex, which contributes to degradation of the retinoblastoma tumor suppressor. *J Virol* 2007; *81* : 9737-47.
44. Pozzebon Maria E, Varadaraj A, Mattoscio D, Jaffray Ellis G, Miccolo C, Galimberti V, *et al*. BC-box protein domain-related mechanism for VHL protein degradation. *Pro Nat Acad Sci* 2013; *110* : 18168-73.
45. Retraction: Ubiquitin/SUMO modification regulates VHL protein stability and nucleocytoplasmic localization. *PLoS One* 2022; *17* : e0265155.
46. Choi SB, Park JB, Song TJ, Choi SY. Molecular mechanism of HIF-1-independent VEGF expression in a hepatocellular carcinoma cell line. *Int J Mol Med* 2011; *28* : 449-54.
47. Jabari M, Allahbakhshian Farsani M, Salari S, Hamidpour M, Amiri V, Mohammadi MH. Hypoxia-Inducible Factor1-A (HIF1α) and Vascular Endothelial Growth Factor-A (VEGF-A) Expression in De Novo AML Patients. *Asian Pac J Cancer Prev* 2019; *20* : 705-10.
48. Sharma A, Sinha S, Shrivastava N. Therapeutic Targeting Hypoxia-Inducible Factor (HIF-1) in Cancer: Cutting Gordian Knot of Cancer Cell Metabolism. *Front Genet* 2022; *13* : 849040.
49. Goel B, Tiwari AK, Pandey RK, Singh AP, Kumar S, Sinha A, *et al*. Therapeutic approaches for the treatment of head and neck squamous cell carcinoma-An update on clinical trials. *Transl Oncol* 2022; *21* : 101426.
50. Hyytiäinen A, Wahbi W, Väyrynen O, Saarilahti K, Karihtala P, Salo T, *et al*. Angiogenesis Inhibitors for Head and Neck Squamous Cell Carcinoma Treatment: Is There Still Hope? *Front Oncol* 2021; *11* : 683570.
51. Lee L-T, Wong Y-K, Chan M-Y, Chang K-W, Chen S-C, Chang C-T, *et al*. The correlation between HIF-1 alpha and VEGF in oral squamous cell carcinomas: Expression patterns and quantitative immunohistochemical analysis. *J Chin Med Assoc* 2018; *81* : 370-5.
52. Bento CF, Fernandes R, Ramalho J, Marques C, Shang F, Taylor A, *et al*. The chaperone-dependent ubiquitin ligase CHIP targets HIF-1α for degradation in the presence of methylglyoxal. *PLoS One* 2010; *5* : e15062.
53. Foxler DE, Bridge KS, Foster JG, Grevitt P, Curry S, Shah KM, *et al*. A HIF-LIMD1 negative feedback mechanism mitigates the pro-tumorigenic effects of hypoxia. *EMBO Mol Med* 2018; *10* : e8304.

For correspondence: Dr Chinmay Kumar Panda, Department of Oncogene Regulation, Chittaranjan National Cancer Institute, Kolkata 700 026, West Bengal, India
e-mail: ckpanda.cnci@gmail.com

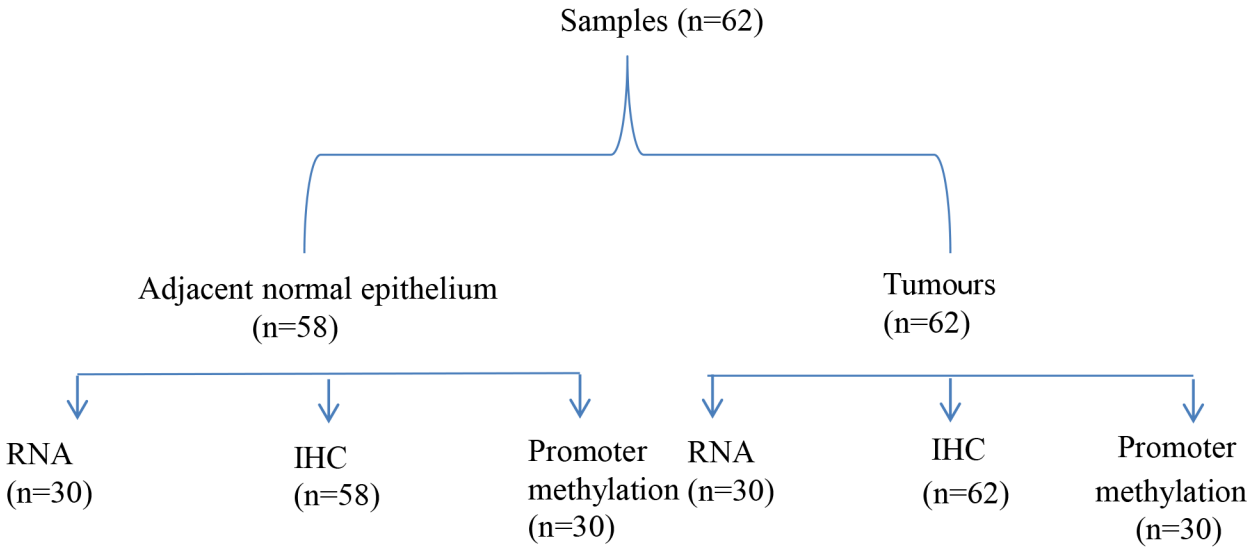

Supplementary Fig. 1. Distribution of the samples used in the study for each of the methods used. IHC, immunohistochemical.

Supplementary Table I. Primer lists used in real-time-PCR and promoter methylation analysis

HPV detection and typing primer

Name of the primer	Purpose of use	Forward primer	Reverse primer	Product size (bp)	PCR condition (°C)
MY09 MY11	HPV detection	5' gcmcagggwcataayaatgg3'	5' cgtccmarrggawactgatc 3'	452 bp	54
E6 region	Detection of HPV 16	5' agggcgtaaccgaaatcgg 3'	5' catatacctcacgtcgca 3'	206 bp	54
LCR region	Detection of HPV 18	5' catatacctcacgtcgca 3'	5' cggttgcataaactatgtat 3'	361 bp	58

RNA primer

Genes	Forward primer	Reverse primer	Product size (bp)	PCR condition (°C)
HIF1α	5'-TTAGAACCAAATCCAGAGTCAC-3'	5'- TATTCACTGGGACTATTAGGCT-3'	125	56
VHL	5'-GCGTCGTGCTGCCCGTATG-3'	5'-TTCTGCACATTTGGGTGGTCTTC-3'	343	62
LIMD1	5'-GTAAATTCATCGGAGGACCTG-3'	5'-CCATCCACAGTCAGCTTG-3'	268	56
VEGF	5'- GAGATGAGCTTCCTACAGCAC-3'	5'- TCACCGCCTCGGCTTGTCACAT-3'	345	59
β2m	5'-GTGCTCGCGCTACTCTCTCT-3'	5'-TCAATGTCGGATGGATGAAA-3'	143	55

Methylation primer

Genes	Forward primer	Reverse primer	Product size	Location
VHL	5'-GAGGTCAAGGCTGCAGTGAG-3'	5'-GAGGCTAGGCCAACTCGTTA-3'	154	292 bp to 140 bp in 5' flanking region
LIMD1	5'-TAGGCAGGTGGAAGTCTTTA-3'	5'-CCAGGTCGTCATACTTATCC-3'	201	30 bp in 5' flanking region to 131 bp within exon 1
K1	5'-TGCCCTCTGGACTGGAACCT-3'	5'-CCTGAGCCCAGCCCAAGTC-3'	445	
K2	5'-AGAGTTTGATGGAGTTGGGT-3'	5'-CATTCGGTTTGGGTCAATCC-3'	229	

HPV, Human papillomavirus; PCR, polymerase chain reaction; HIF1α, hypoxia-inducible factor-1α; VEGF, vascular endothelial growth factor; *VHL*, von Hippel-Lindau; bp, base pairs

Supplementary Table II. Demography of the samples used in real-time-polymerase chain reaction and promoter methylation analysis

Features	n (%)	HPV 16		
		+ve, n (%)	–ve, n (%)	*P*
Total	30	15 (50)	15 (50)	
Primary site				
BM	13 (43)	3 (23)	10 (77)	0.052
TNG	3 (10)	2 (67)	1 (33)	
Oropharynx	10 (33)	8 (80)	2 (20)	
Larynx	4 (13)	2 (50)	2 (50)	
TNM stage				
I	7 (23)	5 (71)	2 (29)	0.24
II	6 (20)	3 (50)	3 (50)	
III	6 (20)	4 (67)	2 (33)	
IV	11 (37)	3 (27)	8 (73)	
Grade				
Mild/WDSCC	18 (60)	11 (61)	7 (39)	0.33
Moderate/MDSCC	6 (20)	2 (33)	4 (67)	
Poor/PDSCC	6 (20)	2 (33)	4 (67)	
Node				
+ve	12 (40)	4 (33)	8 (67)	0.14
–ve	18 (60)	11 (61)	7 (39)	
Tobacco				
+ve	15 (50)	7 (47)	8 (53)	0.22
–ve	15 (50)	8 (53)	7 (47)	

BM, buccal mucosa; TNG: tongue; WDSCC, well differentiated squamous cell carcinoma; MDSCC, moderately differentiated squamous cell carcinoma; PDSCC, poorly differentiated squamous cell carcinoma; –ve, factor absent; +ve, factor present

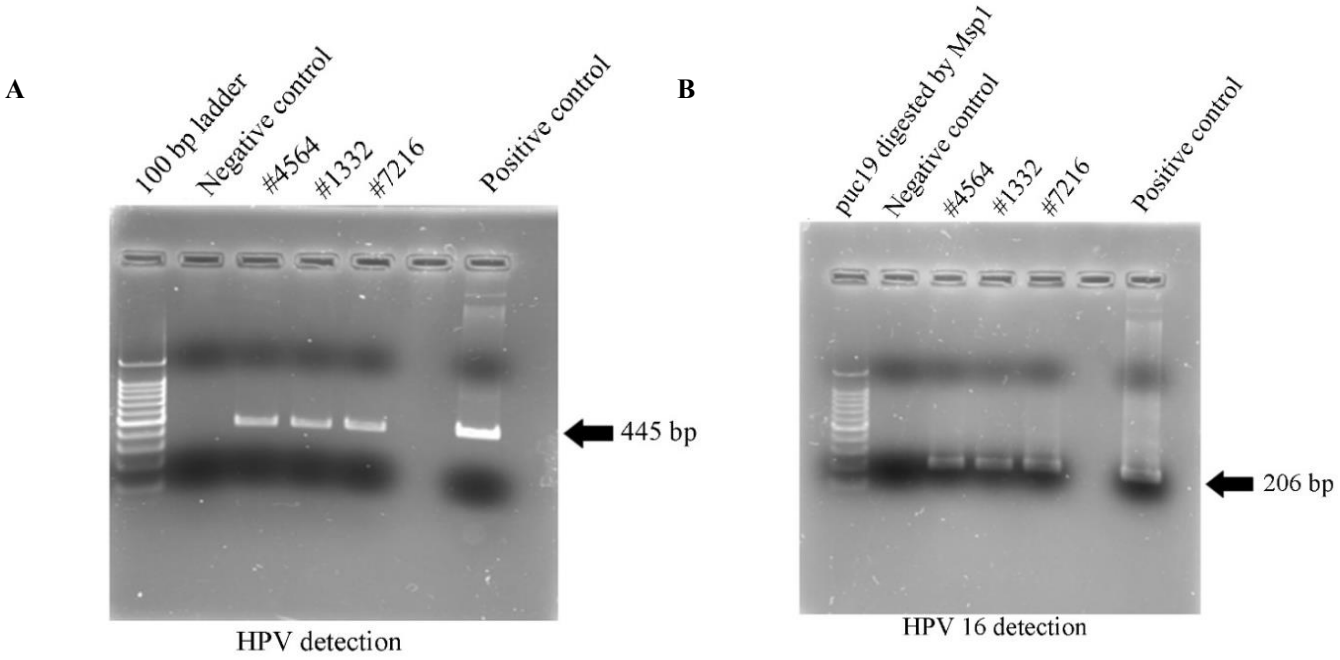

Supplementary Fig. 2. Representative image of human papillomavirus (HPV) infection analysis. (**A**) HPV infection analysis with MY09/MY11 primer set. (**B**) Detection of HPV16 type with primer set from E6 region. HPV, human papillomavirus; bp, basepairs.

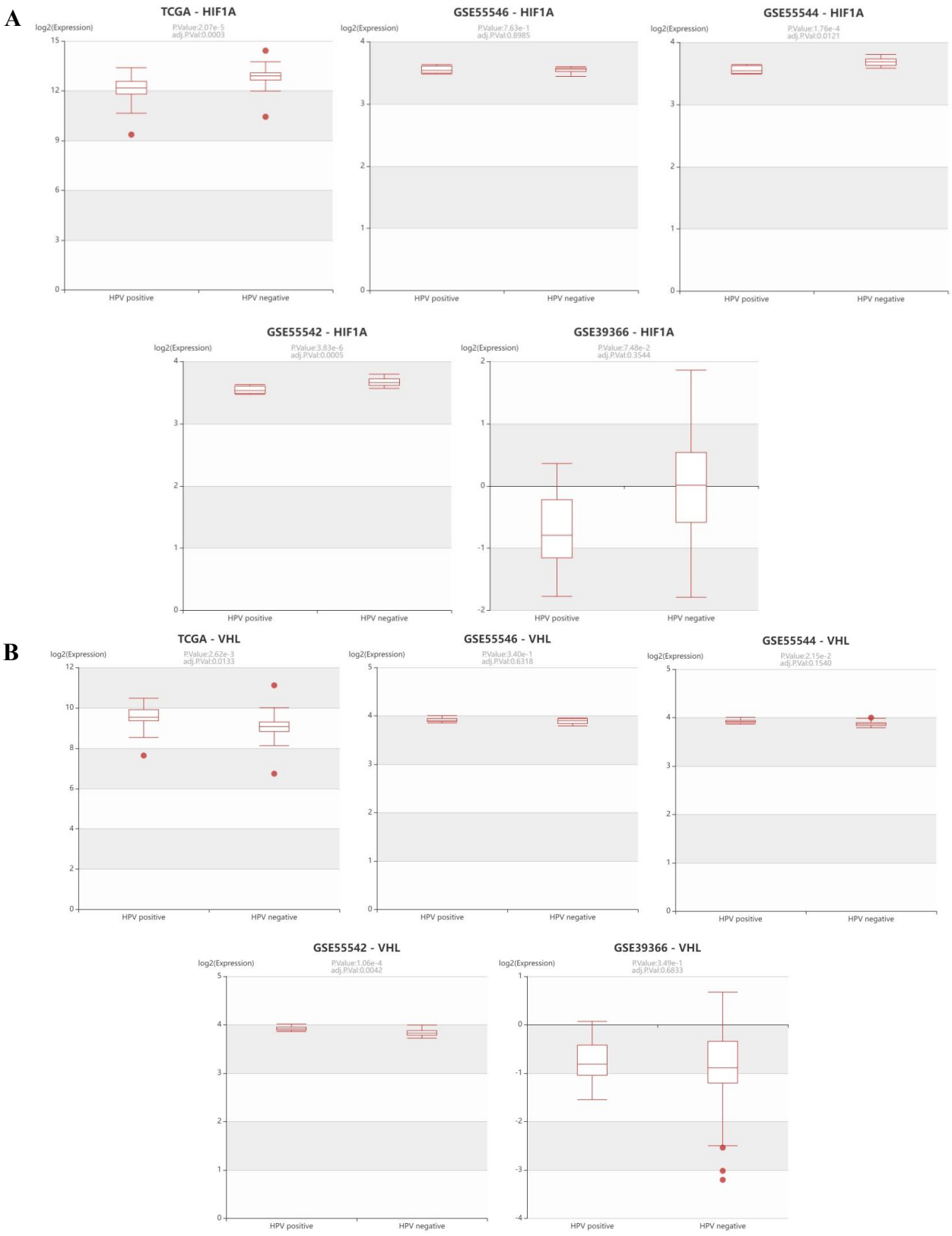

Supplementary Fig. 3. (Contd...)

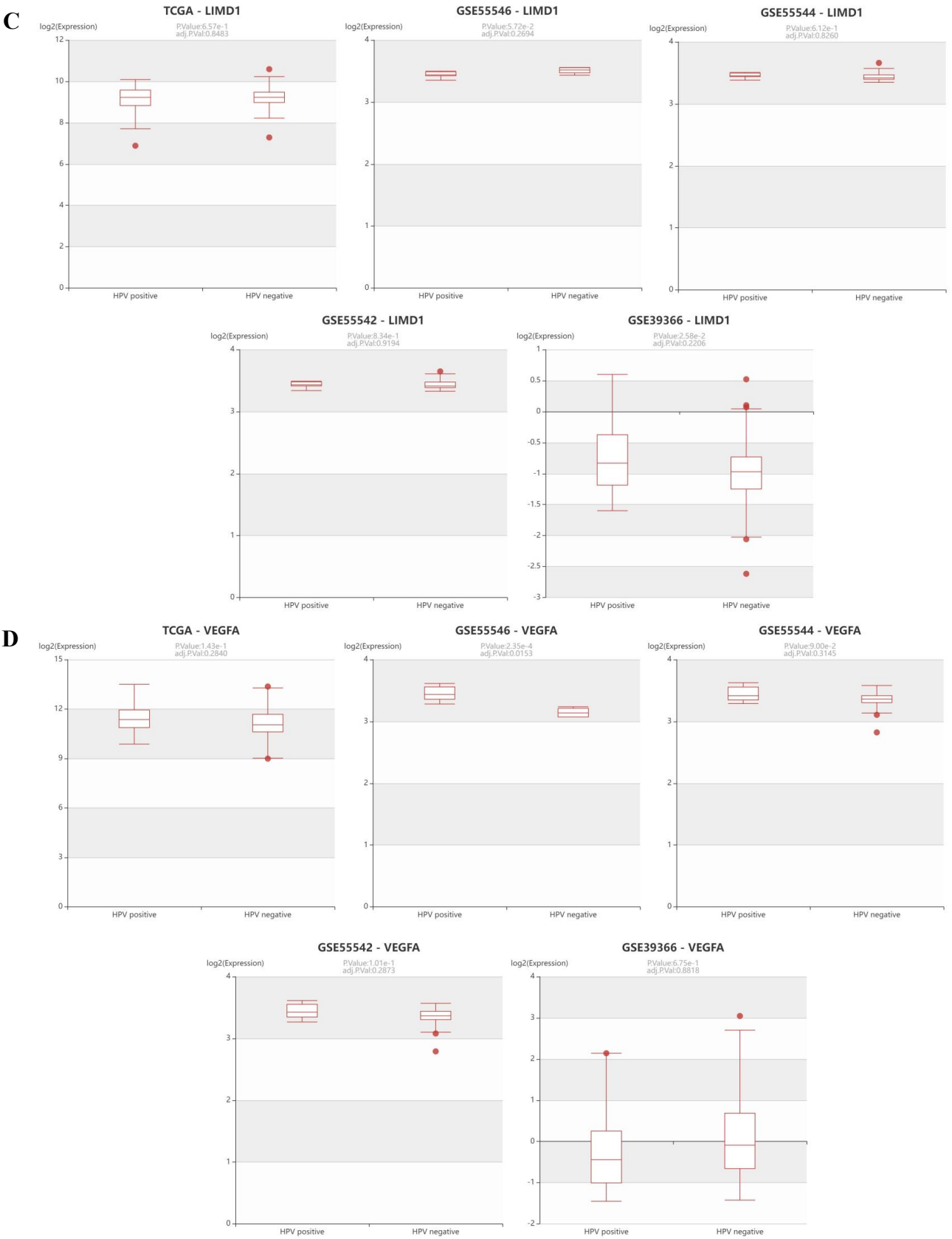

Supplementary Fig. 3. Box plot showing expression pattern of the hypoxia-inducible factor-1α (HIF1α) pathway associated genes in HPV+ve/–ve HNSCC samples in five different datasets along with the *P* value and adjusted *P* values mentioned above the figures. (**A**) HIF1α, hypoxia-inducible factor-1α; (**B**) *VHL*, von Hippel-Landau; (**C**) *LIMD1*, LIM domain containing 1; (**D**) VEGF, vascular endothelial growth factor.

Supplementary Table III. The log fold change of the genes in HPV +ve in comparison to HPV –ve head-and-neck squamous cell carcinoma (HNSCC) samples from different datasets as data mined from HNCDB database *(http://hncdb.cancerbio.info)*

Genes	TCGA (fold change)	*P*	GSE55546 (fold change)	*P*	GSE55544 (fold change)	*P*	GSE55542 (fold change)	*P*	GSE9366 (fold change)	*P*
HIF1α	0.795	2.07E-05	0.11	7.63E-01	–0.123	1.76E-04	–0.126	3.83E-06	–0.7	7.48E-02
VHL	0.479	2.62E-03	0.033	3.40E-01	0.055	2.15E-02	0.097	1.06E-04	–0.61	3.49E-01
LIMD1	–0.068	6.57E-01	–0.064	5.72E-02	0.014	6.12E-01	–0.005	8.34E-01	1.55	2.58E-02
VEGF	0.325	1.43E-01	0.3	2.35E-04	0.118	9.00E-02	0.09	1.01E-01	–0.194	6.75E-01

Supplementary Table IV. The log fold change of the genes' expressions in the HPV +ve and HPV –ve primary head-and-neck squamous cell carcinoma samples used in this study

HIF1α		VEGF		*VHL*		*LIMD1*	
HPV+ve	HPV–ve	HPV+ve	HPV–ve	HPV+ve	HPV–ve	HPV+ve	HPV–ve
0.32	0.17	0.14	0.12	–0.28	–0.18	0.16	–0.13
0.14	0.33	0.11	0.57	–0.01	–0.59	–0.13	–0.20
0.14	0.19	0.1	0.63	–0.19	–0.26	0.18	–0.19
0.41	0.16	0.26	0.18	–0.2	0.06	–0.17	0.02
0.32	0.1	0.19	0.04	–0.12	–0.03	–0.15	–0.28
0.15	0.45	0.18	0.17	–0.13	–0.55	–0.03	–0.05
0.19	–0.01	–0.04	0.15	–0.19	–0.04	–0.32	–0.65
0.96	0.61	0.61	0.69	–0.21	–0.55	0.02	–0.62
0.84	0.08	0.29	0.42	–0.49	–0.81	–0.03	–0.57
1.24	0.63	0.3	1.89	–0.4	–0.27	–0.01	–0.15
0.84	0.41	0.66	0.09	–0.26	–0.38	–0.15	–0.79
0.93	0.56	0.64	1.68	–0.39	–1.12	–0.58	0.14
1.38	1.07	1.84	1.44	0.03	–1.03	0.04	–0.87
0.53	–0.01	1.44	1.62	0.03	–0.09	–1.14	–0.46
1.18	–0.09	1.81	1.29	–1.18	–0.64	–0.02	–0.73
P=0.026		P=0.493		P=0.182		P=0.0833	

Supplementary Table V. The percentage of samples with high/medium protein expression of the genes in HPV +ve and HPV –ve basal/parabasal layers (B/P), spinous layer and HNSCC tissues

Genes	HPV	B/P (%)	Overall B/P (%)	Spinous (%)	Overall spinous (%)	Tumour (%)	Overall tumour (%)
HIF1α	HPV+ve	11/28 (39)	25/58 (43)	6/28 (21)	14/58 (24)	26/30 (87)	43/62 (69)
	HPV–ve	14/30 (47)		8/30 (27)		17/32 (53)	
VHL (N)	HPV+ve	11/28 (39)	31/58 (53)	21/28 (75)	44/58 (76)	3/30 (10)	14/62 (23)
	HPV–ve	20 /30 (67)		23/30 (77)		11/32 (34)	
VHL (C)	HPV+ve	18/28 (64)	43/58 (74)	13/28 (46)	34/58 (59)	14/30 (47)	27/62 (44)
	HPV–ve	25/30 (83)		21/30 (70)		13/32 (41)	
LIMD1 (N)	HPV+ve	19/28 (68)	45/58 (78)	22/28 (79)	45/58 (78)	16/30 (53)	34/62 (55)
	HPV–ve	26/30 (87)		23/30 (77)		18/32 (56)	
LIMD1 (C)	HPV+ve	17/28 (61)	36/58 (62)	13/28 (46)	35/58 (60)	10/30 (33)	19/62 (31)
	HPV–ve	19/30 (63)		22/30 (73)		9/32 (28)	
VEGF	HPV+ve	11/28 (39)	25/58 (43)	4/28 (14)	14/58 (24)	21/30 (70)	38/62 (61)
	HPV–ve	14/30 (47)		11/30 (37)		17/32 (53)	

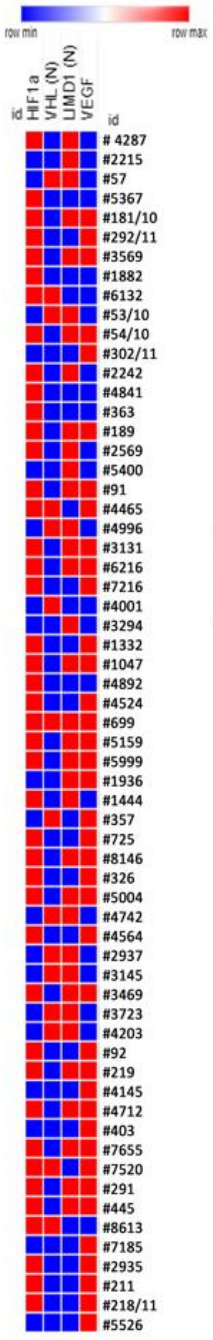

	r	p
HIF1α Vs. VHL	-0.453	0.00023
HIF1α Vs. LIMD1	-0.072	0.58
HIF1α Vs. VEGF	0.3725	0.003

Supplementary Fig. 4. The heatmap represents the expression pattern of HIF-1α, *VHL* and *LIMD1* in the nuclear subcellular location and vascular endothelial growth factor expression in cytoplasmic compartment in the same set of HNSCC samples. The table represents the correlation of the expression pattern among the proteins. The red colour indicates high/medium expression and the blue colour indicates low expression pattern. r, correlation coefficient; *P*, significance level.

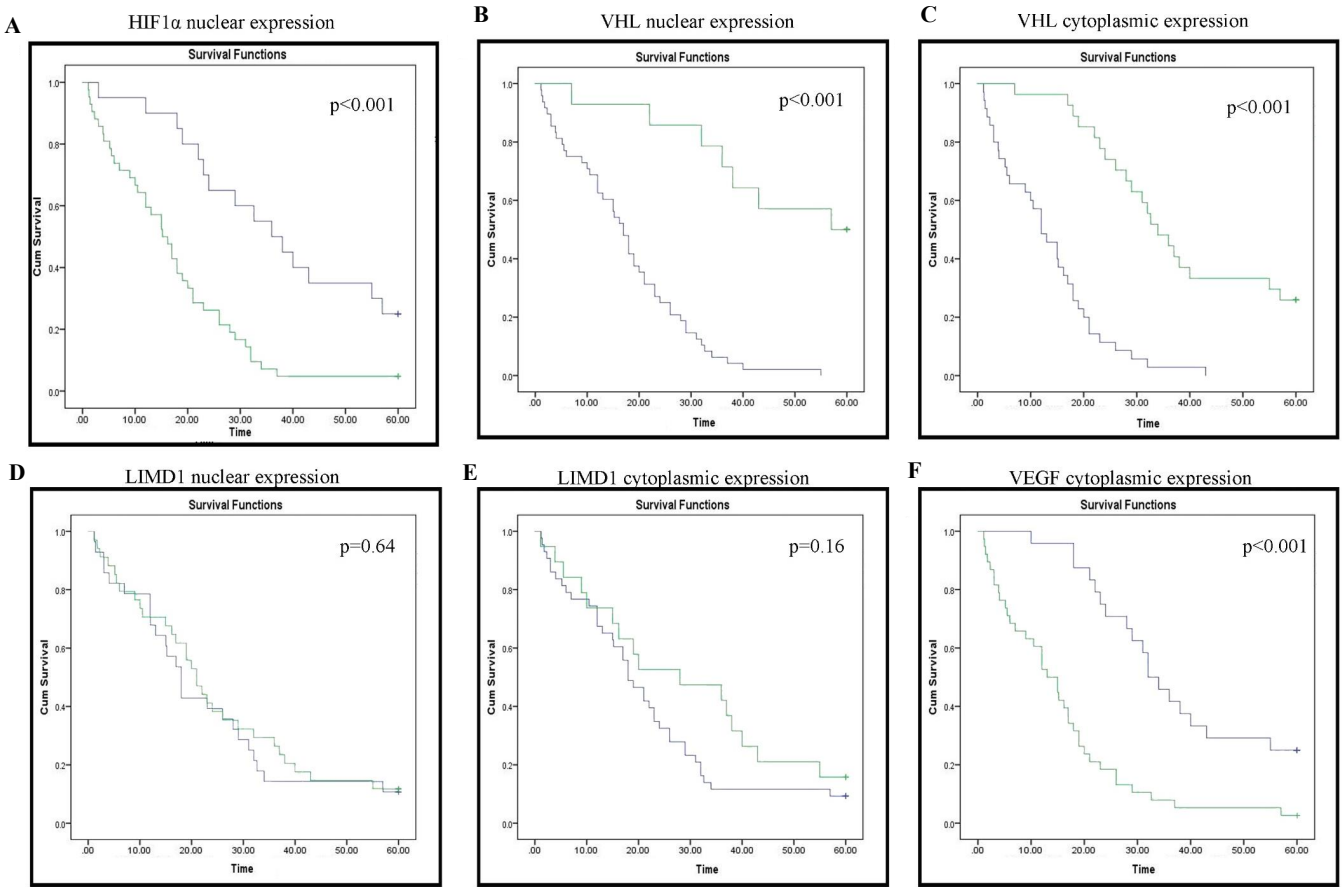

Supplementary Fig. 5. Survival plot showing five years disease-free survival of patients with reference to the expression pattern of the genes in different sub-cellular location. (**A**) HIF1α nuclear expression. (**B** and **C**) *VHL* nuclear and cytoplasmic expression, (**D** and **E**) *LIMD1* nuclear and cytoplasmic expression, (**F**) VEGF cytoplasmic expression. Blue line, low expression; green line, high/medium expression pattern; *(P^{*} <0.001).*

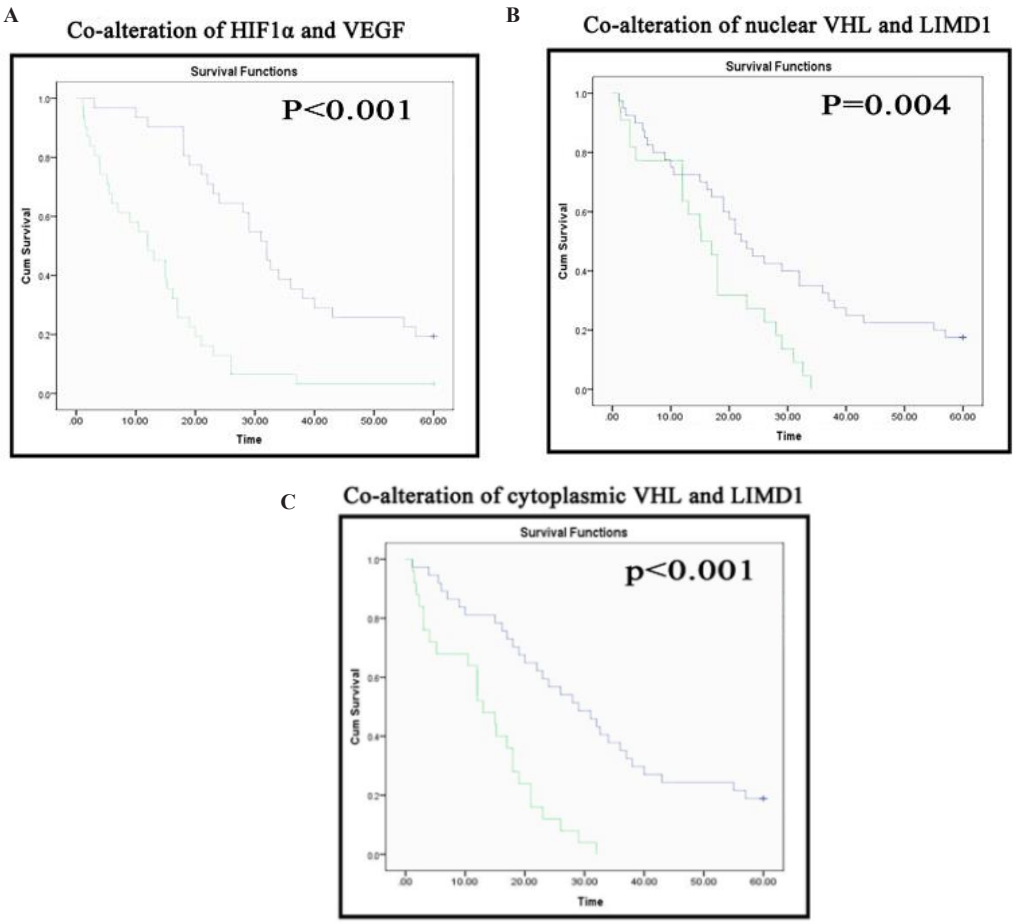

Supplementary Fig. 6. Survival plot with reference to co-alteration of HIF1α/ VEGF and *VHL*/*LIMD*1 genes. Kaplan–Meir analysis, followed by Log Rank test to predict five years disease-free survival of patients with relation to co-expression of genes. (**A**) HIF1α and VEGF co-alteration (blue line, both low or anyone high/medium; green, both high/medium) (**B** and **C**) *VHL* and *LIMD1* co-alteration in nucleus and cytoplasm respectively (blue line, both high/medium or any one low; green, both low) (P^* <0.001).